

Proceedings of the 12<sup>th</sup> International Conference on  
Computational Fluid Dynamics in the Oil & Gas,  
Metallurgical and Process Industries

# Progress in Applied CFD – CFD2017



SINTEF Proceedings

Editors:

Jan Erik Olsen and Stein Tore Johansen

## **Progress in Applied CFD – CFD2017**

Proceedings of the 12<sup>th</sup> International Conference on Computational Fluid Dynamics  
in the Oil & Gas, Metallurgical and Process Industries

SINTEF Academic Press

SINTEF Proceedings no 2

Editors: Jan Erik Olsen and Stein Tore Johansen

**Progress in Applied CFD – CFD2017**

Selected papers from 10<sup>th</sup> International Conference on Computational Fluid Dynamics in the Oil & Gas, Metallurgical and Process Industries

Key words:

CFD, Flow, Modelling

Cover, illustration: Arun Kamath

ISSN 2387-4295 (online)

ISBN 978-82-536-1544-8 (pdf)

© Copyright SINTEF Academic Press 2017

The material in this publication is covered by the provisions of the Norwegian Copyright Act. Without any special agreement with SINTEF Academic Press, any copying and making available of the material is only allowed to the extent that this is permitted by law or allowed through an agreement with Kopinor, the Reproduction Rights Organisation for Norway. Any use contrary to legislation or an agreement may lead to a liability for damages and confiscation, and may be punished by fines or imprisonment

SINTEF Academic Press

Address:       Forskningsveien 3 B  
                  PO Box 124 Blindern  
                  N-0314 OSLO

Tel:             +47 73 59 30 00

Fax:            +47 22 96 55 08

[www.sintef.no/byggforsk](http://www.sintef.no/byggforsk)

[www.sintefbok.no](http://www.sintefbok.no)

**SINTEF Proceedings**

SINTEF Proceedings is a serial publication for peer-reviewed conference proceedings on a variety of scientific topics.

The processes of peer-reviewing of papers published in SINTEF Proceedings are administered by the conference organizers and proceedings editors. Detailed procedures will vary according to custom and practice in each scientific community.

## PREFACE

This book contains all manuscripts approved by the reviewers and the organizing committee of the 12th International Conference on Computational Fluid Dynamics in the Oil & Gas, Metallurgical and Process Industries. The conference was hosted by SINTEF in Trondheim in May/June 2017 and is also known as CFD2017 for short. The conference series was initiated by CSIRO and Phil Schwarz in 1997. So far the conference has been alternating between CSIRO in Melbourne and SINTEF in Trondheim. The conferences focuses on the application of CFD in the oil and gas industries, metal production, mineral processing, power generation, chemicals and other process industries. In addition pragmatic modelling concepts and bio-mechanical applications have become an important part of the conference. The papers in this book demonstrate the current progress in applied CFD.

The conference papers undergo a review process involving two experts. Only papers accepted by the reviewers are included in the proceedings. 108 contributions were presented at the conference together with six keynote presentations. A majority of these contributions are presented by their manuscript in this collection (a few were granted to present without an accompanying manuscript).

The organizing committee would like to thank everyone who has helped with review of manuscripts, all those who helped to promote the conference and all authors who have submitted scientific contributions. We are also grateful for the support from the conference sponsors: ANSYS, SFI Metal Production and NanoSim.

Stein Tore Johansen & Jan Erik Olsen



Organizing committee:

Conference chairman: Prof. Stein Tore Johansen

Conference coordinator: Dr. Jan Erik Olsen

Dr. Bernhard Müller

Dr. Sigrid Karstad Dahl

Dr. Shahriar Amini

Dr. Ernst Meese

Dr. Josip Zoric

Dr. Jannike Solsvik

Dr. Peter Witt

Scientific committee:

Stein Tore Johansen, SINTEF/NTNU

Bernhard Müller, NTNU

Phil Schwarz, CSIRO

Akio Tomiyama, Kobe University

Hans Kuipers, Eindhoven University of Technology

Jinghai Li, Chinese Academy of Science

Markus Braun, Ansys

Simon Lo, CD-adapco

Patrick Segers, Universiteit Gent

Jiyuan Tu, RMIT

Jos Derksen, University of Aberdeen

Dmitry Eskin, Schlumberger-Doll Research

Pär Jönsson, KTH

Stefan Pirker, Johannes Kepler University

Josip Zoric, SINTEF

## CONTENTS

<b>PRAGMATIC MODELLING .....</b>	<b>9</b>
On pragmatism in industrial modeling. Part III: Application to operational drilling .....	11
CFD modeling of dynamic emulsion stability .....	23
Modelling of interaction between turbines and terrain wakes using pragmatic approach .....	29
<b>FLUIDIZED BED .....</b>	<b>37</b>
Simulation of chemical looping combustion process in a double looping fluidized bed reactor with cu-based oxygen carriers.....	39
Extremely fast simulations of heat transfer in fluidized beds.....	47
Mass transfer phenomena in fluidized beds with horizontally immersed membranes .....	53
A Two-Fluid model study of hydrogen production via water gas shift in fluidized bed membrane reactors .....	63
Effect of lift force on dense gas-fluidized beds of non-spherical particles .....	71
Experimental and numerical investigation of a bubbling dense gas-solid fluidized bed .....	81
Direct numerical simulation of the effective drag in gas-liquid-solid systems .....	89
A Lagrangian-Eulerian hybrid model for the simulation of direct reduction of iron ore in fluidized beds.....	97
High temperature fluidization - influence of inter-particle forces on fluidization behavior .....	107
Verification of filtered two fluid models for reactive gas-solid flows .....	115
<b>BIOMECHANICS.....</b>	<b>123</b>
A computational framework involving CFD and data mining tools for analyzing disease in carotid artery .....	125
Investigating the numerical parameter space for a stenosed patient-specific internal carotid artery model.....	133
Velocity profiles in a 2D model of the left ventricular outflow tract, pathological case study using PIV and CFD modeling.....	139
Oscillatory flow and mass transport in a coronary artery.....	147
Patient specific numerical simulation of flow in the human upper airways for assessing the effect of nasal surgery.....	153
CFD simulations of turbulent flow in the human upper airways .....	163
<b>OIL &amp; GAS APPLICATIONS .....</b>	<b>169</b>
Estimation of flow rates and parameters in two-phase stratified and slug flow by an ensemble Kalman filter .....	171
Direct numerical simulation of proppant transport in a narrow channel for hydraulic fracturing application .....	179
Multiphase direct numerical simulations (DNS) of oil-water flows through homogeneous porous rocks .....	185
CFD erosion modelling of blind tees .....	191
Shape factors inclusion in a one-dimensional, transient two-fluid model for stratified and slug flow simulations in pipes .....	201
Gas-liquid two-phase flow behavior in terrain-inclined pipelines for wet natural gas transportation .....	207

<b>NUMERICS, METHODS &amp; CODE DEVELOPMENT .....</b>	<b>213</b>
Innovative computing for industrially-relevant multiphase flows .....	215
Development of GPU parallel multiphase flow solver for turbulent slurry flows in cyclone.....	223
Immersed boundary method for the compressible Navier–Stokes equations using high order summation-by-parts difference operators .....	233
Direct numerical simulation of coupled heat and mass transfer in fluid-solid systems .....	243
A simulation concept for generic simulation of multi-material flow, using staggered Cartesian grids.....	253
A cartesian cut-cell method, based on formal volume averaging of mass, momentum equations.....	265
SOFT: a framework for semantic interoperability of scientific software .....	273
<b>POPULATION BALANCE .....</b>	<b>279</b>
Combined multifluid-population balance method for polydisperse multiphase flows .....	281
A multifluid-PBE model for a slurry bubble column with bubble size dependent velocity, weight fractions and temperature.....	285
CFD simulation of the droplet size distribution of liquid-liquid emulsions in stirred tank reactors .....	295
Towards a CFD model for boiling flows: validation of QMOM predictions with TOPFLOW experiments .....	301
Numerical simulations of turbulent liquid-liquid dispersions with quadrature-based moment methods.....	309
Simulation of dispersion of immiscible fluids in a turbulent couette flow .....	317
Simulation of gas-liquid flows in separators - a Lagrangian approach.....	325
CFD modelling to predict mass transfer in pulsed sieve plate extraction columns .....	335
<b>BREAKUP &amp; COALESCENCE .....</b>	<b>343</b>
Experimental and numerical study on single droplet breakage in turbulent flow .....	345
Improved collision modelling for liquid metal droplets in a copper slag cleaning process .....	355
Modelling of bubble dynamics in slag during its hot stage engineering.....	365
Controlled coalescence with local front reconstruction method .....	373
<b>BUBBLY FLOWS .....</b>	<b>381</b>
Modelling of fluid dynamics, mass transfer and chemical reaction in bubbly flows .....	383
Stochastic DSMC model for large scale dense bubbly flows.....	391
On the surfacing mechanism of bubble plumes from subsea gas release.....	399
Bubble generated turbulence in two fluid simulation of bubbly flow .....	405
<b>HEAT TRANSFER .....</b>	<b>413</b>
CFD-simulation of boiling in a heated pipe including flow pattern transitions using a multi-field concept .....	415
The pear-shaped fate of an ice melting front .....	423
Flow dynamics studies for flexible operation of continuous casters (flow flex cc).....	431
An Euler-Euler model for gas-liquid flows in a coil wound heat exchanger.....	441
<b>NON-NEWTONIAN FLOWS.....</b>	<b>449</b>
Viscoelastic flow simulations in disordered porous media .....	451
Tire rubber extrudate swell simulation and verification with experiments .....	459
Front-tracking simulations of bubbles rising in non-Newtonian fluids.....	469
A 2D sediment bed morphodynamics model for turbulent, non-Newtonian, particle-loaded flows.....	479

<b>METALLURGICAL APPLICATIONS.....</b>	<b>491</b>
Experimental modelling of metallurgical processes .....	493
State of the art: macroscopic modelling approaches for the description of multiphysics phenomena within the electroslag remelting process .....	499
LES-VOF simulation of turbulent interfacial flow in the continuous casting mold .....	507
CFD-DEM modelling of blast furnace tapping .....	515
Multiphase flow modelling of furnace tapholes .....	521
Numerical predictions of the shape and size of the raceway zone in a blast furnace.....	531
Modelling and measurements in the aluminium industry - Where are the obstacles? .....	541
Modelling of chemical reactions in metallurgical processes.....	549
Using CFD analysis to optimise top submerged lance furnace geometries .....	555
Numerical analysis of the temperature distribution in a martensic stainless steel strip during hardening.....	565
Validation of a rapid slag viscosity measurement by CFD.....	575
Solidification modeling with user defined function in ANSYS Fluent.....	583
Cleaning of polycyclic aromatic hydrocarbons (PAH) obtained from ferroalloys plant.....	587
Granular flow described by fictitious fluids: a suitable methodology for process simulations .....	593
A multiscale numerical approach of the dripping slag in the coke bed zone of a pilot scale Si-Mn furnace.....	599
<b>INDUSTRIAL APPLICATIONS .....</b>	<b>605</b>
Use of CFD as a design tool for a phosphoric acid plant cooling pond .....	607
Numerical evaluation of co-firing solid recovered fuel with petroleum coke in a cement rotary kiln: Influence of fuel moisture .....	613
Experimental and CFD investigation of fractal distributor on a novel plate and frame ion-exchanger .....	621
<b>COMBUSTION .....</b>	<b>631</b>
CFD modeling of a commercial-size circle-draft biomass gasifier.....	633
Numerical study of coal particle gasification up to Reynolds numbers of 1000.....	641
Modelling combustion of pulverized coal and alternative carbon materials in the blast furnace raceway .....	647
Combustion chamber scaling for energy recovery from furnace process gas: waste to value .....	657
<b>PACKED BED.....</b>	<b>665</b>
Comparison of particle-resolved direct numerical simulation and 1D modelling of catalytic reactions in a packed bed .....	667
Numerical investigation of particle types influence on packed bed adsorber behaviour .....	675
CFD based study of dense medium drum separation processes .....	683
A multi-domain 1D particle-reactor model for packed bed reactor applications.....	689
<b>SPECIES TRANSPORT &amp; INTERFACES .....</b>	<b>699</b>
Modelling and numerical simulation of surface active species transport - reaction in welding processes .....	701
Multiscale approach to fully resolved boundary layers using adaptive grids.....	709
Implementation, demonstration and validation of a user-defined wall function for direct precipitation fouling in Ansys Fluent.....	717



<b>FREE SURFACE FLOW &amp; WAVES .....</b>	<b>727</b>
Unresolved CFD-DEM in environmental engineering: submarine slope stability and other applications.....	729
Influence of the upstream cylinder and wave breaking point on the breaking wave forces on the downstream cylinder .....	735
Recent developments for the computation of the necessary submergence of pump intakes with free surfaces .....	743
Parallel multiphase flow software for solving the Navier-Stokes equations .....	752
<b>PARTICLE METHODS .....</b>	<b>759</b>
A numerical approach to model aggregate restructuring in shear flow using DEM in Lattice-Boltzmann simulations .....	761
Adaptive coarse-graining for large-scale DEM simulations.....	773
Novel efficient hybrid-DEM collision integration scheme.....	779
Implementing the kinetic theory of granular flows into the Lagrangian dense discrete phase model.....	785
Importance of the different fluid forces on particle dispersion in fluid phase resonance mixers .....	791
Large scale modelling of bubble formation and growth in a supersaturated liquid.....	798
<b>FUNDAMENTAL FLUID DYNAMICS .....</b>	<b>807</b>
Flow past a yawed cylinder of finite length using a fictitious domain method .....	809
A numerical evaluation of the effect of the electro-magnetic force on bubble flow in aluminium smelting process.....	819
A DNS study of droplet spreading and penetration on a porous medium.....	825
From linear to nonlinear: Transient growth in confined magnetohydrodynamic flows.....	831

# MODELLING OF INTERACTION BETWEEN TURBINES AND TERRAIN WAKES USING PRAGMATIC APPROACH

Kjersti Røkenes<sup>1</sup>, Balram Panjwani<sup>2</sup>, Berit Floor Lund<sup>1</sup>, Jon Samseth<sup>2</sup>

<sup>1</sup>Kongsberg Digital, Trondheim, Norway

<sup>2</sup>SINTEF Materials and Chemistry, 7465 Trondheim, NORWAY

\* E-mail: balram.panjwani@sintef.no

## ABSTRACT

Kongsberg Digital (KDI) is currently developing a decision support system for wind farms (Kongsberg EmPower). The objectives of Kongsberg EmPower are to optimize the total power production from a wind farm, forecast the power production and monitor the performance and condition of the wind turbines. Power production from a wind farm depends on the flow field around the wind turbine, which is highly influenced by the interaction between turbine and terrain wakes. Furthermore, increased turbulence due to wake-wake interaction increases structural and fatigue loads on the wind turbine blades, leading to higher operational and maintenance (O&M) cost. An improved understanding on the wake-wake interaction is extremely important for optimizing the power production and for reducing the O&M cost. Performing extensive velocity measurements for an entire wind farm is time consuming and expensive. The traditional approach within wind research and industry has been to use full CFD models when complex flow phenomena have to be taken into consideration, but this is computationally demanding. On the other hand, simple engineering models are unable to capture the interaction of flow over complex terrain and wind turbine wakes. KDI and SINTEF are running a project to develop a fast response simulator with simplified representations of terrain effects and turbine wakes. In the proposed approach a pragmatic model for turbines and terrain wakes interaction is presented. Complex flow over a terrain is estimated with mass consistent model and wake from wind turbine is computed using well established wake models i.e. Jensen and Ainslie model. The pragmatic model for coupling the interaction between turbine wakes and terrain approach is presented. The results obtained from the mass consistent approach are verified with CFD using OpenFoam.

**Keywords:** CFD, OpenFoam, Wakes, Turbines, Terrains

## INTRODUCTION

Wind energy is one of the oldest sources of renewable energy that has been harvested to a large

extent. The current state of turbine technology is mature and available from several manufacturers. The size of the wind turbines is increasing steadily and current size of the wind turbine in terms of power is around 6 MW in operational and up to 10 MW is being developed. Irrespective of the size of the wind turbine, the energy extracted by a wind turbine depends on the local wind conditions. The wind conditions varies significantly from one region to another. Furthermore, local terrain effects can also change the wind conditions and these are significantly different from one site to another. Some countries have relatively flat terrain whereas other countries, i.e. Norway, have very complex terrain. Most of the onshore wind farms in Norway are located in complex terrain and just to name a few: Hundhammerfjellet, Havøygavlen and Hitra Wind Farms. The wind conditions in a complex terrain are relatively harsh and transient in nature. Furthermore, an interaction of wakes generated from a complex terrain with a wind turbine results in increased turbulence and velocity deficit. This leads to reduced power production and higher loads on turbines compared with those located in a flat terrain. The knowledge of the local wind conditions is extremely important for a successful operation of wind farms. The most accurate way to estimate behaviour of such flow is to perform experiments in a full scale wind farm or in reduced scale wind tunnel testing. However, performing experiments on full scale is very challenging and not economically feasible. Wind tunnel testing on a scaled size wind farm is also prohibitive. The other approach is to use numerical simulation of the wind parks.

There are numerous models available for estimating the wind turbine wakes and interaction of wakes generated from neighbouring wind turbines. A review of these models can be found in the review paper by Göçmen (Gocmen et al. 2016) . Similarly there had been some research for estimating the flow over complex terrain (Barthelmie R.J. 2008; Bitsuamlak, Stathopoulos, and Bédard 2004; Cabezón D 2010). Most of the studies performed so far the interaction between turbine and terrain wakes have not caught much attention. One common approach for estimating the wake interaction is to superimpose wake due to

wind turbines and wake due to the complex terrain. This approach is adequate for moderately complex terrain, but not for complex terrain (Cabezón D 2010). The models, except computational fluid dynamics (CFD), developed up to present day for wind farm modelling do not explicitly take into account the complex interaction of flow due to wind turbines and the complex terrain.

The models for flow analysis over a complex terrain can be divided into two categories: "prognostic" and "diagnostic" models (Ratto 1996). Prognostic models solve time dependent mass, momentum and energy conservation equations. Since these models are based on the fundamental of mass, momentum (Navier-Stokes) and energy conservation, they are accurate and descriptive. In the past 50 years, these model has increasingly been developed and applied to wind flow over complex topography. However, the solution of the full set of equations is a computationally demanding task and the cost increases with domain size. Due to their complexity and computational cost, these models are normally run for only a few scenarios to understand the detailed description of the flow i.e. turbulence characteristics and local speed. Brief reviews on assessment of the wind farm performance over complex terrains have been provided by Politis (Politis et al. 2012). According to the authors, one of the major problems with Reynolds-Averaged Navier–Stokes (RANS) approach is turbulence models. These turbulence models have been validated in freestream flow conditions, rather than for atmospheric boundary layer conditions. Nevertheless, Reynolds averaged models predict reasonably accurate overall flow field around the complex terrain. The prognostic models have also been used for verification of simple models. The diagnostic models on the other hand, are based on a simplified approach and do not satisfy all the constraint such as mass, momentum and energy conservation. One of the objectives of the present work is to use these models to verify simple engineering models.

One of the major objectives of the ongoing KonWake project (NFR) is to develop a quasi-real time, user friendly and computationally light simulator for the flow field throughout a wind farm and the near surroundings. The model will be integrated with Kongsberg EmPower, which among other things, will optimize the total power from the wind farm and forecast the power production. SINTEF in collaboration with Kongsberg is developing the wind simulator in EmPower. The wind simulator mainly consists of a simplified model for flow over a complex terrain and turbine wake models. The simulator is designed to simulate wind conditions for a complex terrain in quasi-real time, and therefore it has to be computationally fast and also accurate enough to capture the essential global physics. Wind models for simulating flow over complex terrain based on diagnostic models are chosen due to the relative simplicity. Diagnostic models, either based on linearized Jackson and Hunt (JH) (Jackson and Hunt 1975) theory or mass consistent approaches (Sasaki 1970), are much faster than prognostic models, but the

accuracy is also affected due to unresolved physics. Software such as WAsP (WASP), based on linearized JH theory, predicts the wind accurately when the terrain is sufficiently smooth for the flow to be attached. However, these linear models are not accurate for complex terrain where flow separation dominates. Although some modifications, such as site ruggedness index (RIX) (Troen 1990), has been proposed in order to account for complex geometries, these modifications are still not able to capture the flow field for complex terrain. A wind model based on the mass-consistent approach (Sasaki 1970), satisfying the physical constraints of mass conservation has been chosen in the current research work. Verification of mass consistent model for complex terrain have been performed by Panjwani et al. (Panjwani B. 2015)

## MODEL DESCRIPTION

The mass consistent models are based on the numerical solution of the steady state three-dimensional continuity equation for the mean wind components. The momentum and energy equations are not solved explicitly, but introduced through observed wind data and by adding wake effects in the initial flow field. The mass consistent wind models are attractive for a computationally light simulator for several reasons: 1) they do not require much input data, 2) many simulations for different wind conditions can be performed efficiently 3) Accuracy can be improved via improved initial condition. However, according to Troen (Troen 1990), the JH approach should be preferred compared to the mass-consistent method, due to the fact that it uses more physical constraints than just the continuity equation. An advantage with the mass-consistent models is possibility to add more physical constraints in the initial field. Furthermore, steep slopes affect the JH approach more critically than mass-consistent models (Ratto 1996). The theoretical basis for mass consistent models was developed by Sasaki (Sasaki 1970). Mass consistent models have been applied to many other applications but mostly related to the wind, such as pollutant dispersion in the rural and urban areas where the geometry is complex, fire spreading in forest. Sherman (Sherman 1978) and Ross (Ross et al. 1988) applied mass conservation for understanding the atmospheric flows over complex terrain. Ratto (Ratto 1996) has provided a review on mass-consistent models over complex terrain. In the present work a mass consistent model "Wind 3D" developed by G. Montero et al. (Montero, Montenegro, and Escobar 1998; Wind3D) has been used. A brief theoretical development of a mass consistent model is provided here.

Since the wind model conserves mass, we start with the continuity equation

$$\nabla \cdot \vec{u} = 0 \quad (1)$$

Assuming a field is initialized with an initial condition  $u_0$ , but this initial field does not follow any physical constraint i.e. mass or momentum. Assuming  $\tilde{u}$  is the intermediate field, then the least square

problem is formulated in the computational domain

$$E(\vec{u}) = \int \left[ \alpha_1^2 (\vec{u} - u_0)^2 + (\vec{v} - v_0)^2 + \alpha_2^2 (\vec{w} - w_0)^2 \right] d\Omega \quad (2)$$

The initial conditions,  $u_0$ , can be obtained either from the experimental measurements or from other theoretical methods such as CFD. The constants  $\alpha_1$  and  $\alpha_2$  are the Gauss precision moduli, which are also wind vector-partitioning factors in the horizontal and vertical directions respectively. These parameters are used for velocity adjustment in horizontal and vertical direction. The essential requirement in the mass consistent model is the minimization of the objective function:

$$E(u, v, w) = \min \left[ E(\vec{u}) + \int (\Phi \vec{\nabla} \cdot \vec{u}) d\Omega \right] \quad (3)$$

$$\begin{aligned} u &= u_0 + \lambda_1 \frac{\partial \Phi}{\partial x}; \\ v &= v_0 + \lambda_2 \frac{\partial \Phi}{\partial y} \\ w &= w_0 + \lambda_3 \frac{\partial \Phi}{\partial z} \end{aligned} \quad (4)$$

$$\lambda = [\lambda_1, \lambda_2, \lambda_3] \quad (5)$$

The continuity equation (Eq. 1) and the least square function are inserted in the objective function Eq. 3, which leads to the following equation

$$E(u, v, w) = \int \left[ \alpha_1^2 (\vec{u} - u_0)^2 + (\vec{v} - v_0)^2 + \alpha_2^2 (\vec{w} - w_0)^2 + \lambda \left( \frac{\partial u}{\partial x} + \frac{\partial v}{\partial y} + \frac{\partial w}{\partial z} \right) \right] d\Omega \quad (6)$$

The Lagrange multipliers method (Eq. 4) is employed to minimize Eq. 6, which minimum leads to form the Euler-Lagrange equation.

$$\frac{\partial^2 \Phi}{\partial x^2} + \frac{\partial^2 \Phi}{\partial y^2} + \frac{\partial^2 \Phi}{\partial z^2} = -\frac{1}{\lambda} \left( \frac{\partial u_0}{\partial x} + \frac{\partial v_0}{\partial y} + \frac{\partial w_0}{\partial z} \right) \quad (7)$$

A Dirichlet boundary condition ( $\lambda = 0$ ) at the lateral and top boundaries and the Neumann boundary condition ( $\frac{\partial \lambda}{\partial x} = 0$ ) for the terrain was employed.

The mathematical formulation in the mass-consistent model is a Poisson equation for the Lagrange multiplier (Eq.7) and it is discretised using the finite element method. The accuracy and speed of the model relies on the solution algorithm employed for solving the discretised Poisson equation and on the initial condition. Some common algorithms for solving the Poisson equation are Gauss-Seidel (GS), strongly implicit procedure (SIP), the alternating direction implicit (ADI), the conjugate gradient (CG) and the multigrid approach (Weng, Taylor, and Walmsley 2000). Wind3D

employs, a non-symmetric variant of the classical Conjugate Gradient method, "BICGSTAB", for solving the Poisson equation.

## GENERATION OF INITIAL FIELD

The accuracy of the results obtained from a mass consistent model depends on the initial condition. A most common way to obtain the initial field is to interpolate the 3D field from station data available on the site. The accuracy of the initial field will then be affected by both the accuracy of the station data and the interpolation algorithm. A general procedure for interpolation includes both horizontal and vertical interpolation. A horizontal interpolated velocity field is generated from the few station points, as a function of distance from the stations.

$$u(z) = \varepsilon \frac{\sum_{n=1}^N V_n / d_n^2}{\sum_{n=1}^N 1 / d_n^2} + (1 - \varepsilon) \frac{\sum_{n=1}^N V_n / |\Delta h_n|}{\sum_{n=1}^N 1 / |\Delta h_n|} \quad (8)$$

Where,  $V_n$  is the velocity observed at the  $n^{\text{th}}$  station.  $N$  is the number of stations considered in the interpolation,  $d_n$  is the horizontal distance from station  $n$  to the point in the domain where we are computing the wind velocity,  $|\Delta h_n|$  is the height difference between station  $n$  and the studied point, and  $\varepsilon$  is a weighting parameter which allows the assignment of weights to these interpolation criteria.

A logarithmic velocity profile (Eq.9) is used in vertical interpolation.

$$u(z) = \frac{v^*}{k} \left( \log \frac{z}{z_0} - \Theta \right) \quad (9)$$

The velocity profile (Eq.9) takes into account the friction velocity ( $v^*$ ), the effect of roughness ( $z_0$ ) and the atmospheric stability ( $\Theta$ ). The friction velocity is calculated using the velocities obtained from horizontal interpolation. For further details see the Wind3D manual (Wind3D)

The friction velocities were calculated from the reference plane and reference velocity. The reference plane and reference velocity were estimated from the station data.

## ACCOUNTING OF WAKE EFFECTS IN THE MASS CONSISTENT MODEL

The initial field described in the section above does not account for the local windward and leeward effects explicitly. Measurements data might be consisting implicitly some of effects but not the local effects. For explicitly accounting windward and leeward effects in the initial field, a method proposed by Röckle (Röckle 1990) has been utilized. According to Röckle (Röckle 1990) the flow field around an isolated object generates mainly three regions; displacement zone, cavity zone and wake zone. The displacement zone is established on the windward side of obstacles. The flow in this region might be separated, depending on the slope and aspect ratio of the obstacle on the windward side. The distance

of the displacement zone is determined by the obstacle's dimensions including slope. The cavity zone is the region on the leeward side of the obstacle where the flow separates. The detailed description of the model is provided here [17].

## TURBINE WAKE MODEL

The wake models have been developed for estimating the wake behind the wind turbines. An extensive review of the wake models have been carried out by DTU (Gocmen et al. 2016). Most commonly wake models used for the wake calculation are Jensen, Larsen, Fuga and Ainslie. For the current pragmatic modelling two wake models Jensen and Ainslie are used. Jensen model is one of the most popular models among engineering application due to simplicity. In Jensen model, it is assumed that the wake expanded linearly with a prescribed expansion factor. Modelling of the multiple wind turbine wake interaction is rather straightforward with Jensen model. In the Ainslie mode, the flow behind the turbine is treated in two separate regime, near wake and far wake regime. The near wake regime dominates around 2 to 3 time of rotor diameter from the wind turbine. In the near wake regime, flow expansion mainly take place due to the pressure recovery, and effect of turbulence mixing is not that significant. Ainslie proposed expansion of the wake in the near wake regime based on the experimental data. The wake expansion in the near wake depends on the motor thrust coefficient, ambient turbulence intensity, and wake width. In the far wake regime, pressure effects are not dominating and most of the wake expansion take place due to turbulence mixing. In this region, thin shear Navier stokes equations are solved to obtain both axial and radial velocities.

## WAKE SUPERPOSITION

In the offshore park, power production at any turbine mainly depends on the number of upstream turbines, wind speed and turbulence intensity. Wake produced from the upstream turbine strongly influences the approaching wind speed at the downstream wind turbines. The wake at the downstream turbine is estimating by superimposing the wake from the upstream wind turbines. For wake superposition mainly 2 approaches are used.

Linear Sum

$$\left(1 - \frac{u_{n+1}}{U_\infty}\right) = \sum_{j=1}^n \left(1 - \frac{u_{j+1}}{U_j}\right) \quad 10$$

Quadratic sum

$$\left(1 - \frac{u_{n+1}}{U_\infty}\right)^2 = \sum_{j=1}^n \left(1 - \frac{u_{j+1}}{U_j}\right)^2 \quad 11$$

Where n is the total number of upstream wind turbines and  $u_{n+1}$  is velocity at the downstream wind turbine.  $U_\infty$  is free stream wind speed.  $j$  is an index for  $j^{\text{th}}$  wind turbine.

In onshore wind park the effect of terrain wake is very important. In the present study, the wake superposition approach is extended to account for the terrain wake. In

this model we assumed that wake from the terrain behave similar to the wind turbine wake. The terrain and wind turbine wake interaction is estimated using following approaches.

Linear Sum

$$\left(1 - \frac{u}{U_\infty}\right) = \left(1 - \frac{u_{ter}}{U_\infty}\right) + \left(1 - \frac{u_{tur}}{U_\infty}\right) \quad 12$$

Quadratic sum

$$\left(1 - \frac{u}{U_\infty}\right)^2 = \left(1 - \frac{u_{ter}}{U_\infty}\right)^2 + \left(1 - \frac{u_{tur}}{U_\infty}\right)^2 \quad 13$$

Where subscript ter is used for the terrain and tur is used for the wind turbines.

## VALIDATION OF THE MASS CONSISTENT APPROACH

The validation of the mass consistent approach has been done in an earlier work with Bolund measurement hill data (Panjwani B. 2015). In the current publication, flow over the complex terrain (shown in Figure 1) is performed using CFD and also using mass consistent model. It should be mentioned that the flow over a complex terrain is mainly governed by conservation of mass and momentum for an isothermal system. The mass consistent approach only accounts for the mass conservation, and momentum conservation is not accounted in the mass consistent model. A major difference in the flow fields calculated by CFD and mass consistent models are normally obtained on the leeward and windward side of the hill.

## FLOW SIMULATIONS OF THE TERRAIN

Accurate and reliable flow simulations of wind flow over a complex terrain are important for a wide range of applications, and especially for wind resource assessment and condition monitoring of an operational wind farm. In the present study OpenFoam (OpenFoam 2009) and mass consistent simulation of the entire wind farm located on a complex terrain is carried out. The computational geometry of the complex terrain is based on GIS data with a horizontal resolution of 2 m. The maximum height of the terrain surface is about 300 m above sea level and the extent of the domain is 18 km in the longitudinal direction and 15 km in the lateral direction. The terrain geometry was generated from orography data using MATLAB. The surfaces are discretised with triangular cells that provided the basis for the generation of 3D hexahedral cells for application of the control volume method. The surface geometry of terrain was imported into the OpenFoam pre-processor. The size of the computational box in longitudinal, lateral and normal directions was (18 km x 15 km x 2 km). The mesh was refined close to the terrain surface and the initial mesh includes 2e06 hexahedrons. The accuracy in the results improves with finer mesh. The computational grid (Figure 2) is generated using the TerrainBlockMesher mesh generator (TerrainBlockMesher). A problem with the OpenFoam build-in mesh generator, "snappy hex approach", is generation of unstructured mesh near to the terrain

surface. The mesh on the terrain surface is highly irregular, and this is a major source of numerical error near to the boundary surface. On the other hand TerrainBlockMesher generates high quality of the meshes for the complex geometries. The TerrainBlockMesher first generates a basic mesh, which is mainly an extensive blockMeshDict file consisting of many multi blocks. The number of mesh points for each box is given in the control parameter available with TerrainBlockMesher. This technique allows a large degree of control over the size and shape of the computational cells. This grid technique only uses hexahedral and prismatic cells, and no tetrahedral and pyramid cells. In this case, all cell faces are either vertical or parallel to the underlying terrain surface. This reduces the numerical discretisation errors and allows the use of a second-order discretisation scheme without compromising convergence. This technique has been successfully applied in other CFD studies to model complex urban areas (Peralta et al. 2014).

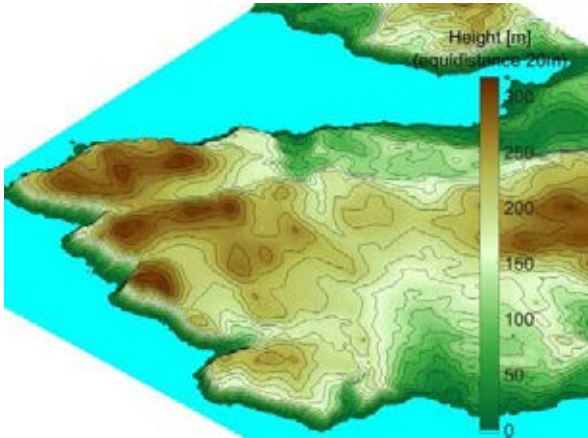


Figure 1: Complex terrain located in Norway

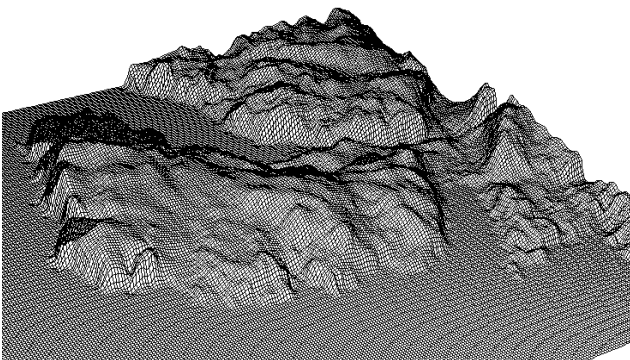


Figure 2: Grid on the terrain using TerrainBlockMesher

### Simulation of the complex terrain

The 3D steady Reynolds-Averaged Navier–Stokes (RANS) equations are solved with the open source CFD code "OpenFoam". The realizable  $k-\epsilon$  model is used for estimating the turbulent kinetic energy and turbulent dissipation. Second-order discretization schemes are used for both the convective and viscous terms of the

governing equations. The SIMPLE algorithm is used for pressure-velocity coupling.

In reality, turbulent kinetic energy and dissipation varies with height above the terrain. The variation in turbulent kinetic energy and dissipation depend on the atmospheric condition. However, in the present study a constant fixed value of turbulent kinetic energy and dissipation rate were used at the inlet of the domain. The inlet turbulent intensity was 0.15 and the turbulent viscosity ratio was 0.2. Furthermore, the default wall functions available in OpenFoam were employed.

### Inlet Boundary condition

A logarithmic boundary condition have been used at the inlet to the boundary of the domain. A logarithm velocity profile, as shown in Figure-3 and described in Eq. (14), is used to approximate the atmospheric boundary layer (ABL).

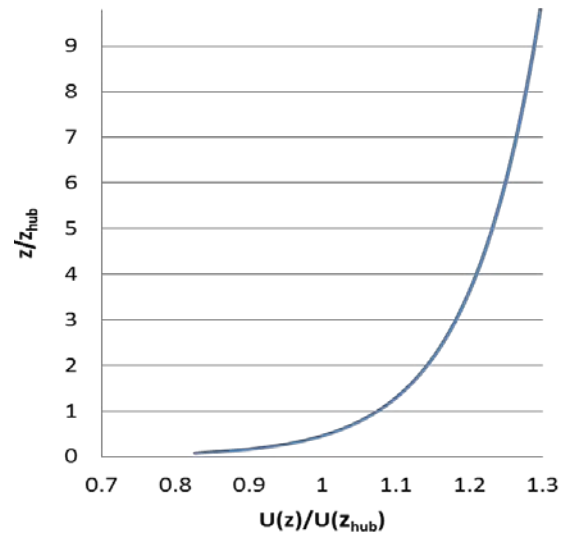


Figure 3 : Vertical profiles of the atmospheric boundary layer (ABL)

$$U = \frac{u_*}{\kappa} \ln\left(\frac{z}{z_o}\right) \quad 14$$

Where  $\kappa$  is the von Kármán constant,  $z$  is height,  $z_o$  is the aerodynamic roughness length and  $u_*$  is the friction wind speed defined by  $\sqrt{\tau/\rho}$ , is the wind stress, and  $\rho$  is air density and  $\tau$  is shear stress at the ground surface.

There are mainly two types of roughness (Blocken 2015); (1) the roughness of the terrain that is included in the computational domain, which is part of the terrain geometry and (2) the roughness of the terrain that is not included in the computational domain i.e.  $z_o$ . This roughness is accounted through boundary layer profile (Eq.14). The knowledge of the roughness  $z_o$  is important because it determines the shape of the inlet profiles of mean wind speed and turbulence properties.

The roughness,  $z_o$  of the surface was around 0.03 m in the current simulations. We have assumed that the selected terrain is relatively smooth and it does not have any dense trees and therefore the chosen roughness should be enough.

A no-slip boundary condition is used on the bottom terrain surface. On the sides and top surface of computational domain a free slip boundary condition is applied. At the exit of the computational domain an outlet boundary condition is used.

## Results and Discussion

CFD studies of flow over complex terrain that consists of an irregular succession of hills and valleys are presented in this section. The CFD data files obtained from the OpenFoam was converted into FLUENT format for visualization purpose. The velocity near to the terrain surface is shown in Figure 4. Dominating flow changes near the terrain surface due to the terrain topography is clearly visible.

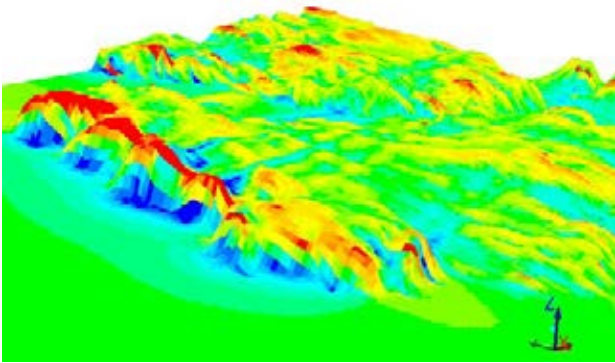


Figure 4: Contour plot of velocity near the terrain surface using OpenFoam

Flow accelerates at the upper edge of the mountain and deaccelerates on the leeward side. A mass consistent simulation of the same terrain was carried out, and a contour plot of the velocity near the terrain surface is shown in Figure 5.

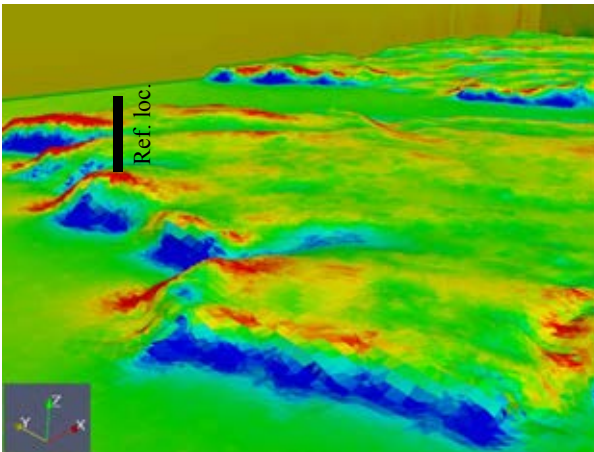


Figure 5: Contour plot of velocity near the terrain surface using mass consistent model

The estimated flow field using both approaches show roughly similar behavior (see Figure 4 and 5). The velocity profile at different downstream positions (along x direction) from reference location is shown in Figure 6, 7 and 8 for mass consistent and CFD results. The reference location is marked in Figure 5. The mass

consistent model under-predicts the velocity at most locations. The reason for this discrepancy is unresolved momentum term in the mass consistent model.

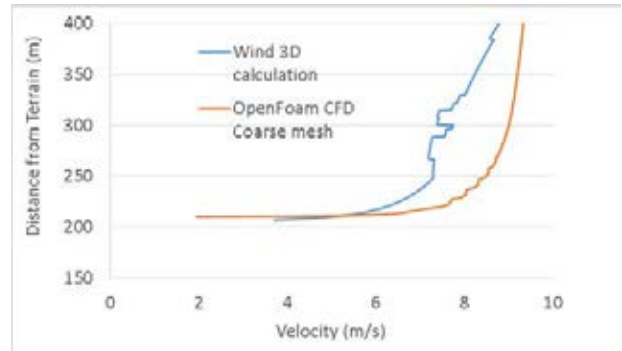


Figure 6: Velocity profile along vertical direction from the terrain surface at reference location (reference location is shown in Figure 5)

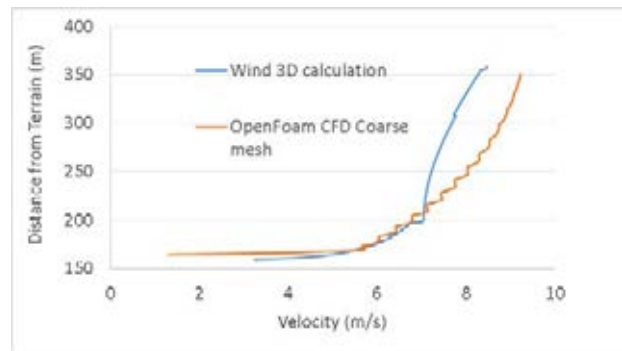


Figure 7: Velocity profile along vertical direction from the terrain surface at 2 km along x direction from reference location (reference location is shown in Figure 5)

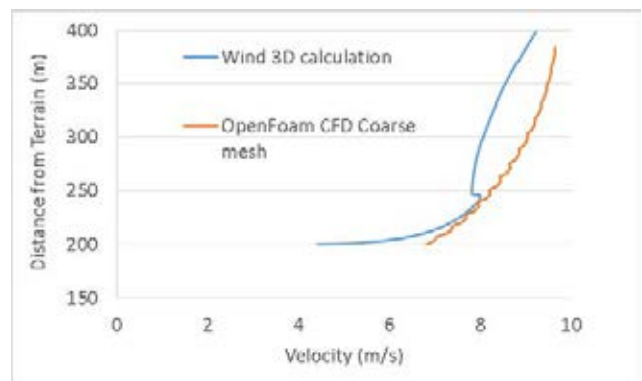


Figure 8: Velocity profile along vertical direction from the terrain surface at 3 km along x direction from reference location (reference location is shown in Figure 5)

Method for coupling the terrain and turbine wake has been described in theory section. In order to verify the approach, a simplified geometrical model setup was generated. In this simplified setup, one small turbine

was mounted on the Bolund hill geometry as shown in Figure 9.

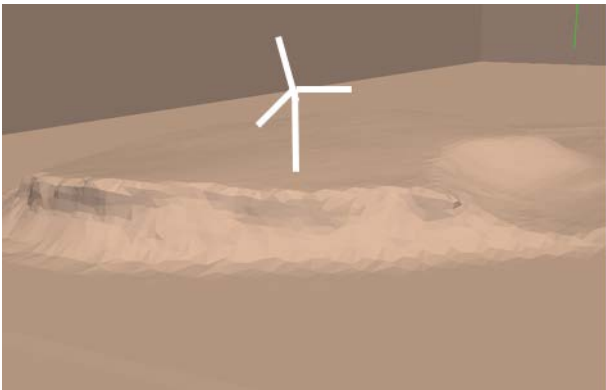


Figure 9: Turbine location on the Bolund terrain

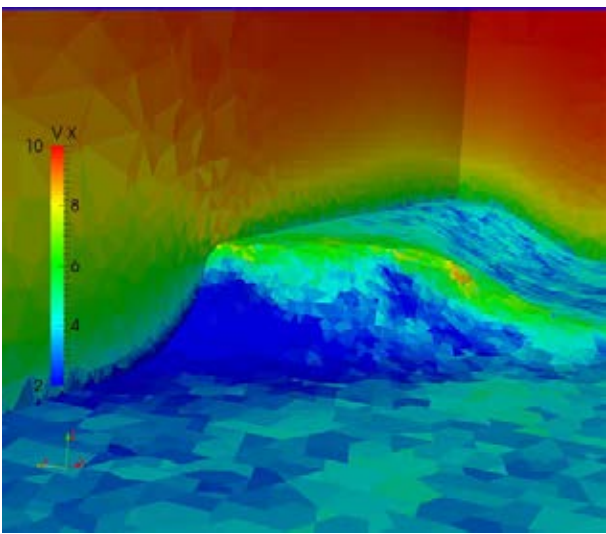


Figure 10: Contour plot of the velocity near the Bolund terrain without wind turbine

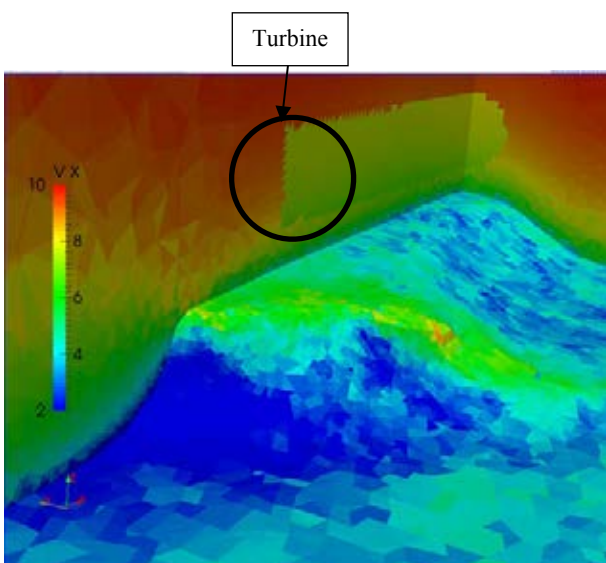


Figure 11: Contour plot of the velocity on the terrain and in turbine cross section

Mass consistent simulation of the Bolund hill without wind turbine was performed and velocity distribution

for this configuration is shown in Figure 10. Wake behind the wind turbine was calculated using Jensen approach. Wake from the wind turbine and wake from the terrain were superimposed using approach described in earlier section. The resulting flow field without wind turbine is shown in Figure 10. The resulting wind flow field due to the turbine and terrain wake interaction is shown in Figure 11. It can be seen that the flow over the terrain interacts with wake generated from the wind turbine. In the present study superposition of terrain and turbine wakes is presented. Verification of the approach is under progress and hopefully, the verification results will be presented in the conference.

## Conclusions

CFD and mass consistent simulations of flow over complex terrain have been carried out. The mass consistent model is able to capture local acceleration and deceleration of flows due to terrain geometry. However, predicted wind velocities using the mass consistent are under-predicted compared with CFD data. The under-prediction of the velocity is mainly due to un-accounting of the momentum equation in the mass consistent model. In the mass consistent model the displacement zone, windward and leeward effects are not considered in the initial field. Accounting for these effects might improve the results. Integration approach of the wind turbine wakes and terrain wake is presented.

## References

- Barthelmie R.J., Frandsen S.T., Rathmann O. , Hansen K. . 2008. "Flow and wakes in large wind farms in complex terrain and offshore." In *EWEA 2008*. Brussels.
- Bitsuamlak, G. T., T. Stathopoulos, and C. Bédard. 2004. 'Numerical Evaluation of Wind Flow over Complex Terrain: Review', *Journal of Aerospace Engineering*, 17: 135-45.
- Blocken, Bert. 2015. 'Computational Fluid Dynamics for urban physics: Importance, scales, possibilities, limitations and ten tips and tricks towards accurate and reliable simulations', *Building and Environment*, 91: 219-45.
- Cabezón D, Hansen KS, . Barthelmie RJ. 2010. "Analysis and validation of CFD wind farm models in complex terrain Effects induced by topography and wind turbines." In *EWEC2010*. Warsaw, Poland.
- Gocmen, T., P. Van der Laan, P. E. Rethore, A. P. Diaz, G. C. Larsen, and S. Ott. 2016. 'Wind turbine wake models developed at the technical university of Denmark: A review', *Renewable & Sustainable Energy Reviews*, 60: 752-69.
- Jackson, P. S., and J. C. R. Hunt. 1975. 'Turbulent wind flow over a low hill', *Quarterly Journal of the Royal Meteorological Society*, 101: 929-55.
- Montero, G., R. Montenegro, and J. M. Escobar. 1998. 'A 3-D diagnostic model for wind field adjustment', *Journal of Wind Engineering and Industrial Aerodynamics*, 74-76: 249-61.



NFR.

<https://www.forskningsradet.no/prosjektbanke/n/#!/project/235754/en>, Accessed 28/04/2017.

- OpenFoam. 2009. *OpenFOAM. The Open Source CFD Toolbox. User Guide* (Free Software Foundation, Inc.).
- Panjwani B. , Lund B.F. Røkenes R., Popescu M. and Samseth J. 2015. "Fast response simulator for flow over a complex terrain: A case study." In *EWEA 2015*. Paris.
- Peralta, C., H. Nugusse, S. P. Kokilavani, J. Schmidt, and B. Stoevesandt. 2014. 'Validation of the simpleFoam (RANS) solver for the atmospheric boundary layer in complex terrain', *ITM Web of Conferences*, 2.
- Politis, E. S., J. Prospathopoulos, D. Cabezon, K. S. Hansen, P. K. Chaviaropoulos, and R. J. Barthelmie. 2012. 'Modeling wake effects in large wind farms in complex terrain: the problem, the methods and the issues', *Wind Energy*, 15: 161-82.
- Ratto, C.F. 1996. "An overview of mass-consistent models. Modeling of Atmosphere Flow Fields." In *D. P. Lalas and C. F. Ratto, Eds, World Scientific Publications*, 379–400.
- Ross, D. G., I. N. Smith, P. C. Manins, and D. G. Fox. 1988. 'Diagnostic Wind Field Modeling for Complex Terrain: Model Development and Testing', *Journal of Applied Meteorology*, 27: 785-96.
- Röckle, R. 1990. 'Determination of flow relationships in the field of complex building structures (in German)', der Technischen Hochschule.
- Sasaki, Yoshikazu. 1970. 'SOME BASIC FORMALISMS IN NUMERICAL VARIATIONAL ANALYSIS', *Monthly Weather Review*, 98: 875-83.
- Sherman, Christine A. 1978. 'A Mass-Consistent Model for Wind Fields over Complex Terrain', *Journal of Applied Meteorology*, 17: 312-19.
- TerrainBlockMesher.  
<https://github.com/jonasIWES/terrainBlockMesher>, Accessed 28/04/2017.
- Troen, I.B. 1990. "A high resolution spectral model for flow in complex terrain." In *Ninth Symposium on Turbulence and Diffusion*. Roskilde.
- WASP. <http://www.wasp.dk/>, Accessed 28/04/2017.
- Weng, W., P. A. Taylor, and J. L. Walmsley. 2000. *J. Wind. Eng. Ind. Aerodyn.*, 86: 169.
- Wind3D. <http://www.dca.iusiani.ulpgc.es/Wind3D/en/>  
Accessed 28/04/2017.